Effects of Nitrogen Substitution in Poly(pyrazolyl)borato Ligands: From Orbital Energy Levels to C–H···O Hydrogen Bonding

Christoph Janiak,* Tobias G. Scharmann, Jennifer C. Green, Richard P. G. Parkin, Mario J. Kolm, Erwin Riedel, Wulfhard Mickler, José Elguero, Rosa M. Claramunt, and Dionisia Sanz

Dedicated to Professor Max Herberhold on the occasion of his 60th birthday

Abstract: The electronic effect of substituting CH with N in poly(pyrazolyl)borato ligands and their transition-metal complexes is shown to be a decrease in energy of the filled metal and ligand orbitals. This conclusion is based on the cyclovoltammograms and photoelectron spectra of bis(hydrotris(azolyl)borato)-iron(II) and -cobalt(II) complexes (azolyl = pyrazolyl and 1,2,4-triazolyl) and on MO calculations. ^{57}Fe Mössbauer spectra of bis(hydrotris(1,2,4-triazolyl)-borato)iron(II) show that there is a fine-tuning of the HOMO–LUMO gap by a shift in transition temperature for the spin equilibrium. ^{15}N NMR spectroscopy supports the assignment of a higher negative charge to the exodentate N-4 nitrogen than to the endodentate N-2 or N-3 positions in the poly(azolyl)borato anions, where azolyl is 1,2,4-triazolyl or tetrazolyl. The electron withdrawing effect of the additional nitrogen atoms and the incorporation of water of crystallization by O–H···N bonding both assist in the formation of (azolyl)C–H···O bonds.

Keywords
cyclovoltammetry · electronic effects · photoelectron spectroscopy · pyrazole ligands · Mössbauer spectroscopy

Introduction

Poly(pyrazolyl)borato anions (**1a** and **2a**) are versatile chelating ligands in the coordination chemistry of transition-metal and main-group elements.[1] They are especially popular as auxiliary ligands in bioinorganic model complexes.[2] The appropriate substitution of the pyrazolyl hydrogen atoms by alkyl or aryl groups to give sterically demanding or so-called "second generation Trofimenko ligands" proved to be crucial in the exploitation of this ligand class for unique chemical transformations and stabilizations and contributed to a resurgence of interest in poly(pyrazolyl)borate chemistry.[1, 3]

In contrast to steric effects from (C–)H → (C–)R substitution, the control and the adjustment of electronic effects in poly(pyrazolyl)borato ligands has hardly been used or investigated. Such an electronic variation could be achieved through the introduction of heteroatoms in the pyrazolyl ring, for example, by a formal (isolobal) C–H → E substitution, where E is a Group 15 element.[4] Despite their interesting potential (the ring heteroatom can be conceived of as a functional group), the resulting poly(1,2,4-triazolyl)borates **1b** and **2b** and the bis-(tetrazolyl)borate **1c**[5] have only recently attracted attention.[7–14] In previous studies we have mainly elaborated on the

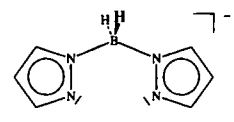

1a

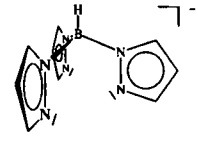

2a

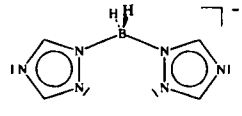

1b

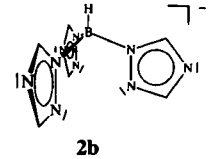

2b

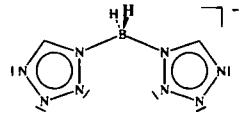

1c

[*] C. Janiak, T. G. Scharmann, M. J. Kolm, E. Riedel
Institut für Anorganische und Analytische Chemie
Technische Universität Berlin
Strasse des 17. Juni 135, D-10623 Berlin (Germany)
Fax: Int. code +(30)314-22168
J. C. Green, R. P. G. Parkin
Inorganic Chemistry Laboratory, South Parks Road, Oxford OX1 3QR (UK)
W. Mickler
Institut für Anorganische Chemie, Universität Potsdam
Postfach 601553, D-14415 Potsdam (Germany)
J. Elguero
Instituto de Quimica Médica, CSIC
Juan de la Cierva 3, E-28006 Madrid (Spain)
R. M. Claramunt, D. Sanz
Departamento de Quimica Orgánica y Biología, UNED
Senda del Rey s/n, E-28040 Madrid (Spain)

0947-6539/96/0208-0992 $ 15.00+.25/0

structural chemistry of **1b**, **2b**, and **1c**. The additional ring nitrogen atoms lead to an interesting coordination chemistry ranging from metal chelates to coordination polymers. Furthermore, the nitrogen atoms that are not utilized for metal coordination tend to engage in hydrogen bonding with water molecules leading to the formation of solvent-stabilized crystal phases with extended water substructures.[8, 10–14]

In the following we want to illustrate how the introduction of additional ring nitrogen atoms affects the properties of the ligands and the central metal by comparing directly the poly(pyrazolyl)- and poly(triazolyl)borate systems with an emphasis on electronic changes.

Results and Discussion

Theoretical Studies on the MOs of Poly(azolyl)borato–Metal Complexes:[*] Qualitative MO studies, performed here as a starting point for the following experimental investigations, show that the main metal–ligand interactions for the tris-chelating azolylborato ligands **2a** and **2b** are indicative of a σ- and π-donor ligand as sketched in Figure 1 for a D_{3d}-symmetrical bis(hydrotris(azolyl)borato)iron complex. The $1e_g^*$ and the a_{1g}^* metal d orbitals (the "t_{2g}" set in octahedral symmetry) are destabilized from non- to weakly antibonding levels by the interaction with the π orbitals of the ligand. Thus, the poly(pyrazolyl)- and poly(triazolyl)borato ligands can be viewed as moderately electron releasing σ-donor and weak π-donor ligands.[15, 16] We note that the extended Hückel MO calculations on **3a** and **3b** show only a small lowering of the energy levels on going from the pyrazolyl to the triazolyl system.[4b] An INDO/S calculation, on the other hand, shows a significant decrease in orbital energies, namely, from −7.9 eV for the HOMO of **3a** to −8.4 eV for that of **3b**. This decrease in energy in **3b** is consistent with a concurrent decrease in energy of the filled ligand π levels (e.g., −5.78 eV for the HOMO of **2a** to −6.39 eV for the HOMO of **2b**, according to an AM1 calculation). Lowering the ligand π-level energy decreases the interaction with the metal

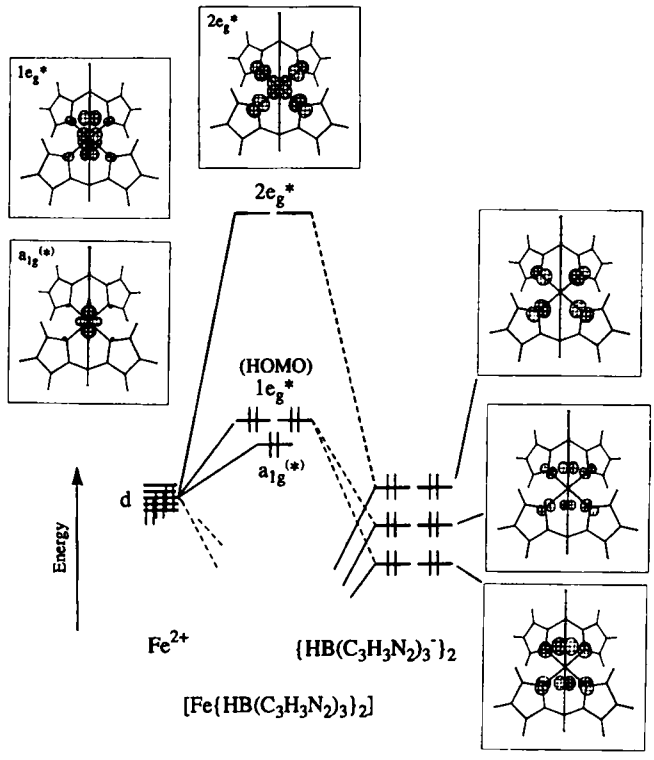

Fig. 1. Schematic molecular orbital diagram for the main metal–ligand interaction of the tris-chelating ligands **2a** and **b** in the iron(II) complexes **3a** and **b**. For clarity, only the contributions of the metal and the nitrogen donor atoms and only one orbital of the degenerate e_g sets are shown in the orbital pictures. The middle azolyl ring in each ligand is pointing perpendicular into or out of the paper plane.

orbitals, such that these will be less destabilized. Hence, the (triazolyl)borato ligands can be considered to be significantly weaker π donors than the (pyrazolyl)borato ligands.

The energy lowering of the nitrogen σ-lone-pair levels in the (triazolyl)borato ligands is less pronounced (ca. 0.2 eV from **2a** to **2b**); still, in the metal complexes the $2e_g^*$ metal–ligand anti-

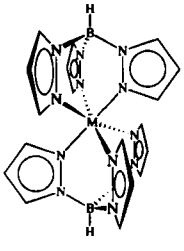

M = Fe **3a**
M = Co **4a**

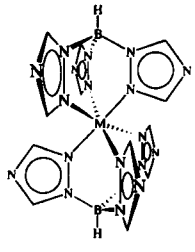

M = Fe **3b**
M = Co **4b**

bonding combination is calculated by the INDO/S method to decrease by 0.4 eV from **3a** to **3b**. Therefore, the (triazolyl)borato ligands are also weaker σ-donor ligands than the (pyrazolyl)borate systems. The decrease in σ- and π-donor strength are also termed "electron-withdrawing" in the following discussions of the experimental results obtained on changing the ligands. Table 1 contrasts selected results of the calculations on **3a** and **3b** with experimental results from the subsequent sections.

Electrochemistry of Bis(hydrotris(azolyl)borato)iron(II) and -cobalt(II) (azolyl = pyrazolyl and 1,2,4-triazolyl): The electro-

Abstract in German: *Mittels Cyclovoltammetrie und Photoelektronenspektroskopie an den Komplexen Bis(hydrotris(azolyl)-borato)eisen(II) und -cobalt(II) (Azolyl = Pyrazolyl und 1,2,4-Triazolyl) sowie MO-Rechnungen wird gezeigt, daß der elektronische Effekt des Ersatzes von CH durch N im Poly(pyrazolyl)-boratoliganden in einer Erniedrigung der Energie der besetzten Metall- und Ligandorbitale besteht. ^{57}Fe-Mößbauer-Spektroskopie an Bis(hydrotris(1,2,4-triazolyl)borato)eisen(II) illustriert eine Feinabstimmung des HOMO–LUMO-Abstandes durch eine Verschiebung der Übergangstemperatur für das Spin-Gleichgewicht. ^{15}N-NMR-Spektroskopie stützt die Zuordnung einer höheren negativen Ladung zur exozähnigen N-4- gegenüber der endozähnigen N-2- oder N-3-Position in den Poly(azolyl)-borat-Anionen mit Azolyl = 1,2,4-Triazolyl und Tetrazolyl. Der elektronenziehende Effekt der zusätzlichen Stickstoffatome, zusammen mit der Einlagerung von Kristallwasser über O–H···N-Brücken, hilft bei der Ausbildung von (azolyl)-C–H···O-Brückenbindungen.*

[*] Three different methods (extended Hückel, INDO/S, and AM1) are used here depending on the compound and the problem. For the transition-metal complexes, the transparent extended Hückel method can be expected to provide a good qualitative understanding of the crystal field splitting, while the spectroscopically parameterized INDO/S method is most likely to best reproduce the orbital-level energies. AM1 as one of the more advanced semiempirical methods was then used for the organic borato ligands.

Table 1. Qualitative comparison of selected experimental and theoretical data for the iron complexes **3a** and **3b** [a].

	INDO/S HOMO/eV	INDO/S LUMO/eV	CV [b] $E_{1/2}$/mV	PE [c] X-Band/eV	UV/Vis [d] $^1A_{1g} \rightarrow {}^1T_{1g}$/nm
3a	−7.9	0.8	185.5	≈7.5	528
3b	−8.4	0.4	920.5	≈8.6	533

[a] We refrained from carrying out calculations on the open-shell cobalt system with its high-spin, $^4T_{1g}$ ground state. [b] Cyclovoltammetry, cf. Table 2. [c] Photoelectron spectroscopy; the low-intensity and large half-width of the X-bands allow only for an approximate assignment, cf. Fig. 3. [d] In view of the large half-width of these electronic transitions, the peak maxima, i.e., the ligand-field splitting, are almost identical. We note that the MO theoretical calculations also give a very similar HOMO–LUMO gap, although the trend of a smaller gap for **3b** is not fully reproduced.

chemistry of bis(hydrotris(pyrazolyl)borato)iron(II) (**3a**) in liquid sulfur dioxide has been described and compared to that of ferrocene and decamethylferrocene.[17] We have carried out cyclovoltammetric investigations on **3a,b** and **4a,b** under less extreme conditions in methylene chloride as a solvent.[18] The results are collected in Table 2. Typical cyclic voltammograms are shown in Figure 2. A truly reversible one-electron process was only observed for **3a**, corresponding to the redox equation $\mathbf{3a} \rightleftharpoons \mathbf{3a}^+ + e^-$. The other compounds gave only quasi-reversible electron processes,[19] based on the difference of the peak potentials, ΔE_p. The very large difference in ΔE_p for **4a** could be due to additional kinetic influences during charge transfer. Also, for the 1+ form of **3b**, partial decomposition may take place, as the cathodic peak current is lower than the anodic peak current (reaching only about 70%) even when taking into account difficulties with the current base-line determination after potential reversal.[19]

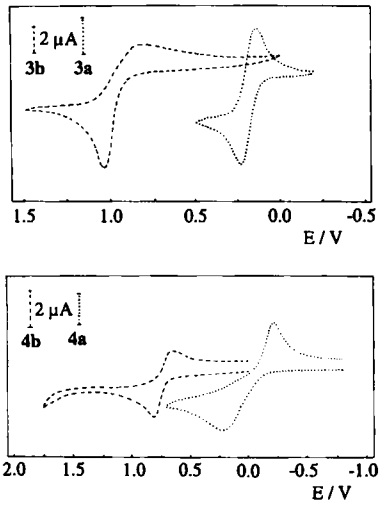

Fig. 2. Cyclic voltammograms at a Pt-disk electrode (2.27 mm²) in CH_2Cl_2 (complex concentration: 10^{-3} mol L^{-1}; 25°C; scan rate 100 mV s^{-1}; 0.1 M [nBu$_4$N][ClO$_4$]).

In the comparison between the (triazolyl)- and (pyrazolyl)-borato complexes, it is important to note that **3b** and **4b** are oxidized and reduced at higher potentials than their pyrazolyl analogues **3a** and **4a**. Hence, the (triazolyl)borate metal compounds are more difficult to oxidize, and the oxidized form is more readily reduced to the neutral complex than the pyrazolyl-based system with the same metal. The differences between the half-wave potentials ($E_{1/2}$) of the iron and cobalt complexes are essentially identical (735 mV between **3a** and **3b**; 722 mV between **4a** and **4b**). Consequently, an increase in redox potentials corresponds to a decrease in orbital energy for the highest occupied level (cf. Table 1). This orbital energy decrease in turn must be due to the weaker π-donor character of the triazolyl compared to the pyrazolyl moiety (see above).

Photoelectron Spectroscopy of Bis(hydrotris(azolyl)borato)-iron(II) and -cobalt(II) (azolyl = pyrazolyl and 1,2,4-triazolyl): A study of the photoelectron spectra of the sodium and thallium complexes as well as of the homoleptic transition-metal complexes with M = Fe, Co, Ni, Cu, and Zn have been described in the literature for the hydrotris(pyrazolyl)borato ligand **2a**.[22, 23] The difference between the tris(pyrazolyl)- and the tris(triazolyl)borato ligands, **2a** and **2b**, is the presence of a nitrogen atom instead of a C–H group in each of the three ring systems in the latter. The three extra nitrogen lone pair orbitals in **2b** will give rise to additional bands in the lower energy region of the spectrum (at the expense of the higher energy region). The He I photoelectron spectra of the tris(triazolyl)borato complexes of iron and cobalt, **3b** and **4b**, together with the spectra of the analogous tris(pyrazolyl)borato complexes **3a** and **4a**, for comparison, are displayed in Figure 3 (the He II PE spectra have been collected as well, but are not shown here; see below). Owing to the D_{3d} symmetry of the complexes, the six nitrogen lone pairs give rise to molecular orbitals which transform as $A_{1g} + A_{2u} + E_g + E_u$.

Several observations can be made about the appearances of the He I spectra of **3b** and **4b**. Firstly, the onset bands (X) and the main ligands peaks (A, B, and C) in the tris(triazolyl)borate spectra occur at higher ionization energies than in the corresponding tris(pyrazolyl)borate spectra: the onset of Band A at about 10 eV is approximately 2 eV higher than in the tris(pyrazolyl)borate spectra. The reason for this is that the triazolyl group is more "electron withdrawing" than the pyrazolyl group, that is, the orbital levels lie at lower energy (cf. Table 1). It is noteworthy that this "electron withdrawing" effect is also visible in a comparison of the PE spectra of pyrazole and triazole.[24]

Secondly, the shape of Band A in the tris(triazolyl)borate spectra is significantly different to the shape of Band A in the

Table 2. Summary of voltammetric parameters for the oxidation of [M{HB(C$_3$H$_3$N$_2$)$_3$}$_2$] (M = Fe **3a**, Co **4a**) and [M{HB(C$_2$H$_2$N$_3$)$_3$}$_2$] (M = Fe **3b**, Co **4b**) in CH_2Cl_2 [a].

	E_{pc}/mV [b]	E_{pa}/mV [b]	$E_{1/2}$/mV [c]	ΔE_p/mV [d]	n [e]	Remarks
3a in liq. SO_2	−150	−102	−126	48	0.99	from ref. [17] [f]
3a in MeCN			280			from ref. [20] [g]
3a in CH_2Cl_2	200	260	230	60		from ref. [21] [h]
3a	139	232	185.5	93	1.03	reversible one-electron process
3b	810	1031	920.5	221	0.67	quasi-reversible one-electron process
4a	−217	213	4	430	0.93	quasi-reversible one-electron process
4b	641	811	726	170	1.27	quasi-reversible one-electron process

[a] 0.1 M [nBu$_4$][ClO$_4$]; T = 25°C, reference Ag/AgCl, unless noted otherwise. [b] Cathodic and anodic peak potentials. [c] $E_{1/2} = (E_{pa} + E_{pc})/2$. [d] Difference between the anodic and cathodic peak potentials, $\Delta E_p = E_{pa} - E_{pc}$. [e] Number of transferred electrons, $n = i_{pa}/i_{pc}$. [f] 0.1 M [nBu$_4$N][PF$_6$]; T = −40°C. The oxidation *and* the reduction of the electrogenerated species **3a**$^+$ were studied in ref. [15], with only E_{pc} given for the reduction wave. E_{pa} of the reduction wave was calculated from ΔE_p = 48 mV; reference Ag quasi-reference electrode, Pt working electrode. [g] 0.1 M [Et$_4$N][ClO$_4$]; reference Ag/AgCl in MeCN. [h] 0.1 M [nBu$_4$N][ClO$_4$]; reference saturated calomel electrode; based on the potential difference of E(Ag/AgCl) − E(SCE) = 44 mV in aqueous solution, comparative values of 156, 214 and 186 mV would be obtained for E_{pc}, E_{pa}, and $E_{1/2}$, respectively, for **3a** from ref. [21].

0947-6539/96/0208-0994 $ 15.00+.25/0 Chem. Eur. J. 1996, 2, No. 8

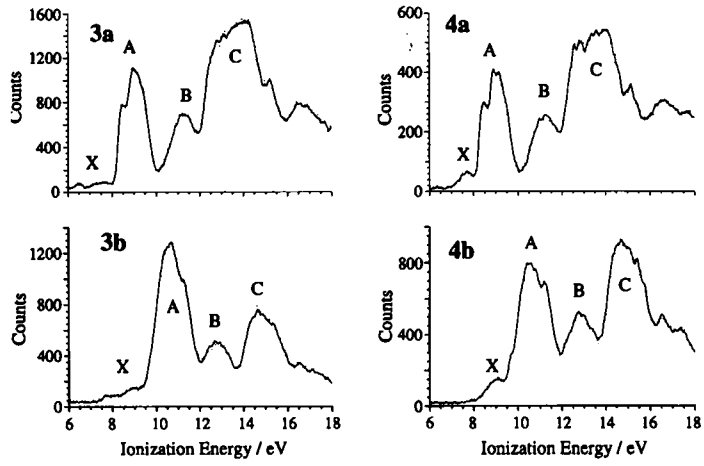

Fig. 3. He I photoelectron spectra of **3b** and **4b**, and of **3a** and **4a**, for comparison

tris(pyrazolyl)borate spectra. There is a distinct shoulder on the high ionization side of the peak of the former, which is not observed in the latter. This is due to one of the extra bands attributed to the ring nitrogens mentioned earlier. AM1 calculations place the nitrogen lone-pair ionizations at the high-energy side of the ring π band. It is also noted that a distinct shoulder is visible on the lower ionization energy side of Band A in the tris(pyrazolyl)borate spectra, but this band is not so well resolved in the tris(triazolyl)borato complexes.

Further observations can be made by comparison of the He I and He II spectra (not shown here) of a given compound. Firstly, the B+C band has a higher relative intensity in the He I spectra of both iron and cobalt complexes than in the corresponding He II spectra. This is because the band is due to the ionization of σ electrons, which have a higher photoelectron cross-section with respect to ionizing radiation of lower energy. Secondly, the onset bands (X) at low ionization energy (up to 8 eV in the pyrazolyl- and up to 9.5 eV in the triazolylborato complexes) show a slightly higher relative intensity in the respective He II spectra; this indicates that the ejected electrons have a higher photoelectron cross-section with respect to the higher energy He II radiation, and are therefore metal d electrons.

Spin-Equilibrium and Temperature-Variable (UV/Vis, DSC, and ^{57}Fe Mössbauer) Studies of Bis(hydrotris(azolyl)borato)iron(II) (3b): In the iron complexes of tris(azolyl)borato ligands the magnitude of the magnetic moment shows a dependence on temperature due to a temperature-dependent equilibrium between the diamagnetic $^1A_{1g}$ low-spin state and the paramagnetic $^5T_{2g}$ high-spin state with four unpaired electrons (Fig. 4).[11, 20, 25–32] Furthermore, in substituted bis(poly(pyrazolyl)borato)iron(II) complexes, the magnetic moment was found to vary strongly with substitution.[16, 33] The interplay of the steric effects of substituents with the different sizes of the low- and high-spin Fe^{II} ions was demonstrated to be the decisive factor in controlling the relative stability of the spin states.[26, 32] The

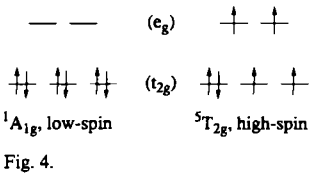

Fig. 4.

transition temperature $T_{1/2}$ (50% low- and high-spin state) for **3a** was given at about 133 °C (405–407 K) upon heating.[29]

A temperature-variable UV/Vis spectroscopic study and a differential-scanning calorimetry (DSC) measurement on **3b** (Fig. 5), as well as a temperature-variable ^{57}Fe Mössbauer study gave a transition temperature of about 65 °C. The decrease in transition temperature from **3a** to **3b** corresponds to a destabilization of the low-spin state in the latter. As the steric requirements in the ligands **2a** and **2b** are the same, the destabilization must be of electronic origin such that the ligand field strength is smaller in the (triazolyl)borato ligand **2b**. The change in the ligand field splitting from **3a** to **3b** must be quite small, however, as judged by the similarity of d–d transition wavelength in the UV/Vis spectra of **3a** and **3b**. A direct comparison of the UV/Vis spectra (measured in CH_2Cl_2) gives $\lambda = 528$ nm for **3a**[34] and 533 nm for **3b** (conc. 3 mg mL^{-1} in each case).

The temperature-variable ^{57}Fe Mössbauer study on a powdered sample of **3b** between 17 and 136 °C (heating and cooling) shows a reversible and rather steep phase change without hysteresis (see Table 3 and Fig. 6).[28] A singlet absorption is observed at temperatures below 62 °C/335 K with an isomer shift, $\delta^{\alpha-Fe}$, in the range of 0.40–0.44 mm s^{-1} and with practically no quadrupole splitting ($\Delta E_Q \approx 0$–0.16 mm s^{-1}). This indicates the presence of octahedrally coordinated iron(II) with a symmetrical

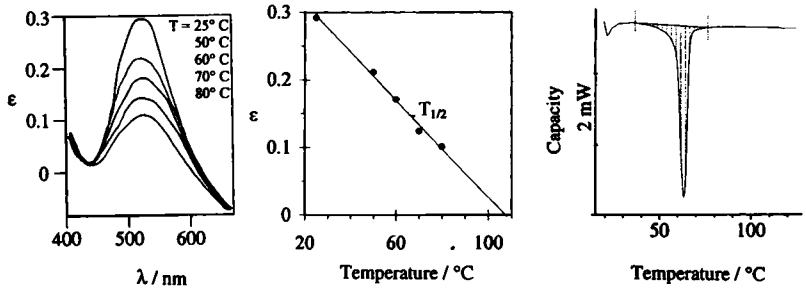

Fig. 5. Sequence of temperature-variable UV/Vis spectra from 25 to 80 °C in the range of the d–d transition for **3b** in aqueous solution as absorption vs. wavelength (left) and intensity vs. temperature (middle), and DSC diagram for **3b** (right). The extinction coefficient in the UV/Vis spectra are scaled with the zero value to the tail of the charge-transfer band. Integration of the DSC curve gives $\Delta H = 17.1$ kJ mol^{-1} and $\Delta S = (\Delta H/T_{1/2})$ 51 J K^{-1} mol^{-1} [24] (heating rate 10 K min^{-1}).

electron configuration, t_{2g}^6, in the low-spin singlet state ($^1A_{1g}$).[31] The small change in $\delta^{\alpha-Fe}$ for $^1A_{1g}$-Fe^{II} in the temperature range between 17 and 62 °C is due to the inverse dependency between the isomer shift and temperature.

The singlet indicative of the Fe^{II} low-spin ($^1A_{1g}$) state is transformed within a few degrees (335–345 K or 62–72 °C) for the most part into the doublet of the Fe^{II} high-spin ($^5T_{2g}$) form. In comparison to the singlet, the doublet has a higher isomer shift ($\delta^{\alpha-Fe} \approx 0.95$ mm s^{-1}) and a very large quadrupole splitting of $\Delta E_Q \approx 3.30$ mm s^{-1}. With increasing temperature (up to 136 °C/409 K), $\delta^{\alpha-Fe}$ also decreases slightly (to 0.92 mm s^{-1}) while ΔE_Q increases further (to 3.50 mm s^{-1}). The parameters of this doublet line correspond to octahedrally coordinated high-spin Fe^{II}, in the $^5T_{2g}$ quintet state. A comparison of the respective low- and high-spin complexes with the same ligand shows that the isomer shift usually decreases as spin pairing takes place. The large value of ΔE_Q is due to the asymmetric $t_{2g}^4 e_g^2$ electron configuration.[31] The details of the spin transition will be the subject of some future work including a high-temperature Mössbauer study up to the decomposition temperature of **3b**.

In Table 3 the parameters of the low- and high-spin components of **3b** are compiled and compared to those of **3a**. The parameters of the low- and high-spin components of **3a** and **3b**

Table 3. Parameters of ^{57}Fe Mössbauer spectra for the iron complexes **3a** and **3b** (cf. Fig. 6).

Compd	Ref.	$(T\pm\Delta T)$/K [θ/°C]	$\pm v$ [a]/mm s^{-1}	N_{lin} [b]	$\delta^{\alpha-Fe}$ [c]/mm s^{-1}	$\Gamma/2$ [d]/mm s^{-1}	ΔE_Q [e]/mm s^{-1}	A_r/% [f] (A/Ages)	State
3a	[26]	4.2 [−269]	(6.0)	1	+0.48	0.13	0.22	100	$^1A_{1g}$
		293 [+20]	(6.0)	1	+0.40	0.14	0.20	100	$^1A_{1g}$
3a	[30]	295 [+22]		1	+0.41	0.14	0.20	100	$^1A_{1g}$
3a	[29] [h]	295 [+22]	5.0	2 a)	+0.43	0.19 [g]	0.17 [g]	98	$^1A_{1g}$
				b)	+0.94	0.19 [g]	3.55	2	$^5T_{2g}$
		410 [+137]	5.0	2 a)	+0.32	0.19 [g]	0.17 [g]	31	$^1A_{1g}$
				b)	+0.80	0.19 [g]	2.91	69	$^5T_{2g}$
3b	[26]	293 [+20]	(6.0)	1	+0.32	0.10	0.07	100	$^1A_{1g}$
3b	this work	290±2 [+17]	2.0	1	+0.44	0.15	0.15	100	$^1A_{1g}$
		319±2 [+46]	2.0	1	+0.43	0.17	0.12	100	$^1A_{1g}$
		335.0±0.5 [+61.8]	4.0	1	+0.40	0.34	0.002	100	$^1A_{1g}$
		339.0±0.5 [+65.8]	4.0	2 a) [i]	+0.26	0.85	0.00 [g]	64	$^1A_{1g}$
				b)	+0.94	0.40	3.16	36	$^5T_{2g}$
		342.0±0.5 [+68.8]	4.0	2 a) [i]	+0.26	1.30	0.00 [g]	50	$^1A_{1g}$
				b)	+0.96	0.41	3.20	50	$^5T_{2g}$
		344.5±0.5 [+71.3]	4.0	2 a) [i]	+0.26	1.36	0.00 [g]	42	$^1A_{1g}$
				b)	+0.96	0.35	3.26	58	$^5T_{2g}$
		349±1 [+76]	4.0 [j]	1	+0.95	0.33	3.28	(100)	$^5T_{2g}$
		379±1 [+106]	4.0 [j]	1	+0.93	0.20	3.46	(100)	$^5T_{2g}$
		409±2 [+136]	4.0 [j]	1	+0.92	0.16	3.51	(100)	$^5T_{2g}$

[a] Measuring velocity. [b] Number of lines used to fit the spectrum. [c] Isomer shift refered to α-iron at room temperature. [d] $\Gamma/2$ is half of the half-width value Γ. Data from ref. [26,29,30] were converted herein. [e] Quadrupole splitting. [f] Line area relative to total area. [g] Parameter was fixed during the fit operation. [h] Temperature-variable study in the range of 295–430 K [29]; examples of some selected measurings. [i] The fitting program, which is based on Lorentzian curves, combines the additional depth in the left arm of the asymmetric doublet with the singlet, thereby causing an artificial isomer shift and line broadening (see also [j]). [j] For reasons of simplicity this spectrum was fitted with a doublet line only, although a singlet line still contributes to the spectrum. At present we are not able, however, to satisfactorily include the asymmetry of the doublet owing to relaxation in the fitting routine. Inclusion of the singlet would only lead to an unreasonable isomer shift value of around −0.40 mm s^{-1} (!) together with large line widths as the program combines the additional depth in the left arm of the doublet with the singlet.

are very similar; this suggests a similar chemical environment for both iron nuclei. Mössbauer spectroscopy is, in principle, well suited for a study of the electronic environment of the resonant nucleus (here: iron). The isomer shift ($\delta^{\alpha-Fe}$) is a direct function of the s electron density at the nucleus, but is also influenced indirectly by shielding/screening effects of the p and d electrons on the s electrons. An increase in $\delta^{\alpha-Fe}$ indicates a decrease in the electron density at the absorber, that is, a decrease in the number of valence 4s electrons for iron, or an increase in the number of screening 4p and 3d electrons.[31]

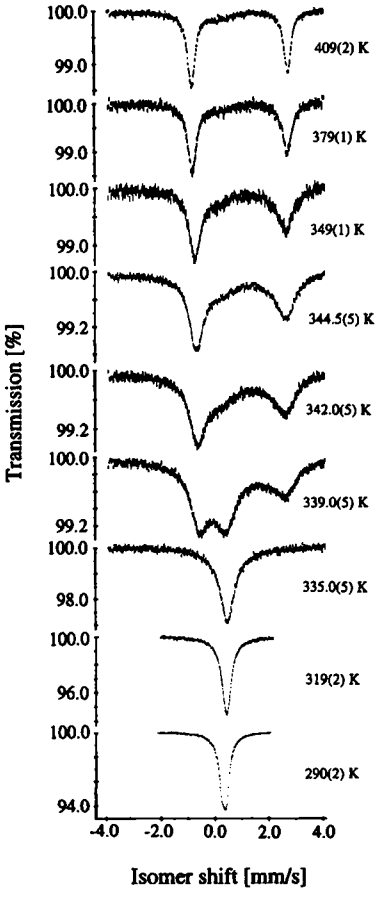

Fig. 6. ^{57}Fe Mössbauer spectra of **3b** as a function of temperature. The isomer shift is scaled to the shift of α-Fe as origin of the ordinate.

We explain the small difference in $\delta^{\alpha-Fe}$ between the high-spin isomers of **3a** (0.85 mm s^{-1} at 430 K) and **3b** (0.92 mm s^{-1} at 409 K) by a difference in bonding character: the (pyrazolyl)borato ligand **2a** forms more covalent bonds. An increase in covalent character will result in an effective decrease in 3d shielding, because of additional delocalization towards the ligands. The result is a decrease in shift.

NMR of the Potassium Salts of the Poly(azolyl)borato Ligands 1b, 2b, and 1c: ^{15}N NMR chemical shifts are an extremely sensitive monitor of the electronic environment of the nitrogen atom. The ^{15}N NMR spectra of the poly(azolyl)borato anions were therefore collected in order to gain information on the relative charge distribution and the donor properties of the nitrogen atoms. The results of the poly(triazolyl)borate compounds **1b** and **2b** and the bis(tetrazolyl)borate **1c** together with the known NMR data of the poly(pyrazolyl)borates **1a** and **2a**[15] are reported in Table 4. The assignment of the different nitrogen atoms is straightforward.[15, 35] The introduction of an additional nitrogen atom into the pyrazolyl rings at position 4 results in a slight increase in the shielding of N-2 by about 7 ppm for **1a** → **1b** and 14 ppm for **2a** → **2b** (Fig. 7).

The same effect is observed in ^{15}N NMR studies of substituted azoles.[35, 37] A small shielding effect of about 1–2.5 ppm is also found for the pyrrole-type nitrogen atom N-1. The introduction of a fourth nitrogen at the N-3 position in the tetrazolylborate system leads to a strong deshielding of the neighboring N-2 and N-4 positions (cf. Fig. 7). The magnitude of deshielding of around 73 and 78 ppm, respectively, is rather similar for both 1,2-interactions, again in line with studies of neutral azoles.[37]

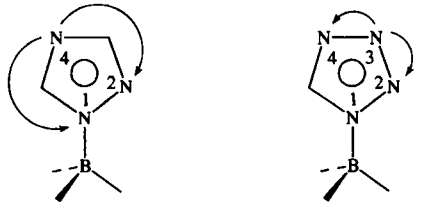

Fig. 7.

0947-6539/96/0208-0996 $ 15.00+.25/0 Chem. Eur. J. 1996, 2, No. 8

Table 4. ^{15}N NMR chemical shifts (δ) [a] and $^{1}H-^{15}N$ coupling constants (Hz) [b] of (pyrazolyl)borates **1a** and **2a**, (triazolyl)borates **1b** and **2b**, and (tetrazolyl)borate **1c**.

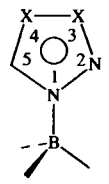

X = CH, N

Compd	Solvent	N-1	N-2	N-3	N-4	Ref.
1a	[D$_6$]DMSO	−137.3 ^3J(H-3) = 7 ^3J(H-4) = 7	−70.4 ^2J(H-3) = 13	–	–	[15]
2a	[D$_6$]DMSO	−141.9 ^3J(H-3) = 8 ^3J(H-4) = 8	−68.8 ^2J(H-3) = 13	–	–	[15]
2a	D_2O	n.o. [c]	−86.2 ^2J(H-3) = 13			this work
1b	[D$_6$]DMSO	−138.0 ^2J(H-5) = 14	−77.2 ^2J(H-3) = 15	–	−133.1 ^2J(H-3,5) = 13	this work
1b	D_2O	n.o.	−91.4 ^2J(H-3) = 16	–	−140.6	this work
2b	[D$_6$]DMSO	−144.1	−80.4	–	−132.0	this work
2b	D_2O	−147.4 ^2J(H-5) = 18	−92.5 ^2J(H-3) = 15	–	−141.2 ^2J(H-3,5) = 13	this work
1c	[D$_6$]DMSO	−124.4	−4.1	−11.2	−54.7	this work
1c	D_2O	−124.1 ^2J(H-5) = 10	1.4 ^3J(H-5) = 5	n.o.	−64.3 ^2J(H-5) = 14	this work

[a] From nitromethane external reference; negative shifts are to high frequency (upfield), implying an increased shielding. Note that the sign notation is reversed from the one used in ref. [35]. The spectra in D_2O were originally measured against a saturated aqueous solution of $^{15}NH_4{}^{15}NO_3$ with $\delta(NH_4) = -359.5$ from neat CH_3NO_2. [b] $^1H-^{15}N$ coupling constants in DMSO have been measured only for **1b**. [c] n.o. = not observed; possibly due to their broad resonance because of quadrupolar coupling and relaxation effects from the boron atom [36].

This leaves us with the question of how the nitrogen chemical shift or its variation translates into the electron density or its variation at the nitrogen atom. This question is not easily answered. The electron charge density enters both the local diamagnetic and paramagnetic shielding term for the nuclear screening constant. Thus, a dependence of the nitrogen chemical shifts on the charge densities in related compounds can often be rationalized; however, the role of the charge term, which can be further subdivided into σ and π charge densities, should not be overemphasized.[38, 39] Generally a higher negative charge on the nitrogen atoms corresponds to an increased shielding when comparing nitrogen atoms of a similar type (e.g., N-4) or different nitrogen atoms in the same compound (e.g., in **2b** or **1c**).[38] A fair agreement between the NMR chemical shift and the AM1-calculated charge is indeed observed for the N-2 and N-4 nitrogen atoms of the (pyrazolyl)- and (triazolyl)borato ligands, however, not for those of the (tetrazolyl)borato ligand. We note that a simple chemical shift–atomic charge correlation for ^{15}N encompassing compounds that are not closely related is usually not very satisfactory.[39, 40]

To account for the difference in chemical shifts of the (tetrazolyl)borato anion **1c** the excitation energy may be important. The paramagnetic shielding term depends in a reciprocal manner on the excitation energies, $\Delta E_{i\rightarrow j}$, of low-lying $\sigma,n \rightarrow \pi^*$ transitions. Often this quantity is replaced by an average excitation energy, ΔE_{av}, which is assumed to be constant throughout a group of related molecules, or represented in crude approximation by the lowest-energy electronic transition, or the HOMO–LUMO gap.[39] According to an AM1 calculation, the HOMO–LUMO gap is indeed not very different for **1a,b** and **2a,b** (it only varies between 10.24 and 10.44 eV), but increases appreciably for **1c** (11.13 eV). An increase in ΔE would correspond to a decrease in shielding.

Finally, we note that hydrogen-bonding effects are quite pronounced for pyridine-type nitrogen atoms, because of the exposure of their lone-pair electrons to interactions with the solvent environment. The formation of hydrogen bonds from solvent molecules to pyridine-type nitrogen atoms in pyrazoles or imidazoles results in a considerable increase (an upfield shift) in nitrogen shielding with a concomitant smaller upfield shift for the pyrrole resonance N-1 in pyrazoles and a downfield shift for the N-1 resonance in imidazoles.[35, 41] Similar hydrogen-bonding effects can be seen here in the (azolyl)borato anions when comparing the chemical shifts in DMSO and in D_2O in Table 4. Both, the N-2 and N-4 nitrogen in the (triazolyl)borates **1b** and **2b** show an upfield shift in D_2O, with a smaller shielding increment for N-1. It is unclear whether the different magnitudes in chemical shift for N-2 and N-4 upon changing the solvent from DMSO to D_2O might be related to the probability, preference, or strength of hydrogen-bond formation to the two different nitrogen atoms. From observations in the transition-metal chemistry of **1b** and **2b**, the exodentate N-4 nitrogen atom was deduced to be the stronger donor atom giving the more stable metal–ligand interaction.[14]

For the bis(tetrazolyl)borate **1c**, on the other hand, only the resonance N-4 is shifted upfield, while N-1 remains essentially invariant and N-2 experiences a downfield shift. Maybe this is an indication that the N-4 nitrogen atom is more prone to hydrogen-bond formation, in line with the observation that only the N-4 nucleophile functions as a donor atom towards transition metals in the complex formation.

Concluding this section, we find that the nitrogen NMR chemical shifts provide useful information concerning the electronic differences between the endo- and exodentate N-2 and N-4 nitrogen donor atoms. The NMR studies support our earlier assignment that N-4 has a higher negative net atomic charge and electrostatic potential than N-2 in **2a**, **2b**, and **1c**.[10, 12] The fact that the tris(triazolyl)borato ligand **2b** uses N-2 instead of the more "basic" N-4 nitrogen to coordinate to metals like iron, cobalt, nickel, copper, and zinc has been explained by the chelate effect together with the ligand-field stabilization energy.[14] Otherwise, neutral 1*H*-1,2,4-triazole and tetrazole coordinate to metal centers by the N-4 donor atoms.[42, 43]

From the above studies we can, however, not say much concerning the electronic effect exerted by the additional N-4 on the N-2 nitrogen and the change in N-2 donor properties. The nitrogen chemical shift values are not easily interpreted in terms of the expected electron withdrawing effect. Perhaps this information as well as additional support for the N-4/N-2 comparison can be obtained from the series of the *N*-methylpyrazole, -triazole, and -tetrazole heterocycles. The basicity of these derivatives (expressed by their pK_a values) increases from tetrazole (−3.00) over pyrazole (2.06) to triazole (3.20).[44a] The protonation site was found to be (as expected) N-2 for *N*-methylpyrazole, and N-4 for *N*-methyltriazole and -tetrazole.[44] As a consequence, *N*-methyltriazole is more basic than the pyrazole analogue when it protonates on N-4. Assuming that the effect of the N-4 nitrogen atom in *N*-methyltriazole is like that of a nitro substituent in the 4-position in *N*-methylpyrazole, the pK_a value for N-2 in the triazole could be taken as that of *N*-methyl-4-nitropyrazoles, namely, −2.18. Nothing is known about the basicity of tetrazole when it protonates at N-2, but it has to be a weaker base than N-4 as judged from the protonation site. To summarize, the basicity of N-2, which is somewhat related to the ability to share its lone pair, decreases very rapidly from

N-methylpyrazole (2.06) over *N*-methyltriazole (ca. −2.2) to *N*-methyltetrazole (below −3.0).

With respect to the magnitude of the electron withdrawing effect exerted by the different azolyl residues when bound to a metal, a comparison of the Hammett σ_p shielding constants for *N*-methylpyrazole (0.28), -triazole (0.45), and -tetrazole (0.58) may also be illustrative.[45] The numbers indicate that the electron withdrawing effect increases in the order pyrazole < triazole < tetrazole. A pyrazolyl residue is like a halogen (σ_p for Cl: 0.24, Br: 0.26), hence it has also been called a pseudohalogen, while triazolyl is more like -COMe ($\sigma_p = 0.47$) and tetrazolyl like $-CF_3$ ($\sigma_p = 0.53$).

Table 5 reports the ^{13}C NMR chemical shifts and some $^1H-^{13}C$ coupling constants determined for compounds **1b**, **2b**, and **1c**, together with relevant data from the literature. In line with

Table 5. ^{13}C NMR chemical shifts (δ) and ^1H and ^{13}C NMR coupling constants (Hz) of (pyrazolyl)borates **1a** and **2a**, (triazolyl)borates **1b** and **2b**, and (tetrazolyl)borate **1c** (for numbering see Table 4).

Compd	Solvent	C-3	C-4	C-5	Ref.
1a	D_2O	141.3	105.6	137.1	[15]
		$^1J = 181.8$	$^1J = 174.9$	$^1J = 183.9$	
		$^2J = 7.2$	$^2J = 10.3$		
		$^3J = 7.2$	$^2J = 10.3$		
2a	D_2O	141.9	106.0	135.7	[15]
		$^1J = 182.6$	$^1J = 175.8$	$^1J = 186.1$	
		$^2J = 7.2$	$^2J = 10.2$	$^2J = 6.8$	
		$^3J = 7.2$	$^2J = 10.2$	$^3J = 4.4$	
				$^3J(BH) = 2.4$	
1b	[D$_6$]DMSO	151.2	–	147.6	this work
		$^1J = 199.4$	–	$^1J = 202.7$	
		$^3J = 11.5$	–	$^3J = 7.8$	
				$^3J(BH) = 4.0$	
1b	D_2O	152.4	–	149.2	[13]
1b	none (CPMAS)	153.6	–	149.8	this work
				150.7	
2b	[D$_6$]DMSO	151.7 [a]	–	147.3 [a]	[9]
2b	[D$_6$]DMSO	151.7	–	147.4	this work
		$^1J = 201.3$	–	$^1J = 205.0$	
		$^3J = 11.6$	–	$^3J = 7.9$	
2b	D_2O	152.8	–	148.6	[11]
2b	none (CPMAS)	153.1	–	149.0	this work
		154.0	–	149.6	
1c	[D$_6$]DMSO	–	–	147.5	this work
				$^1J = 210.6$	
1c	D_2O	–	–	148.5	[7]
1c	none (CPMAS)	–	–	150.1	this work
		–	–	152.0	

[a] Unassigned.

our preceding discussion, the introduction of nitrogen atoms at positions 3 and 4 increases both the ^{13}C chemical shifts and the $^1J(^1H-^{13}C)$ coupling constants (both phenomena are related, but not in a linear way). The effect of N-4 on the $^1J(^1H-^{13}C)$ coupling constants is about 18 Hz (cf. **1a** and **1b**, C-3 and C-5), and that of N-3 about 8 Hz (cf. **1b** and **1c**, C-5). There is also a small increase in $\delta(^{13}C)$ (about 1 ppm) as well as in $^1J(^1H-^{13}C)$ (between 1 and 2 Hz) when [D$_6$]DMSO is replaced by D_2O. This increase can be related to the interaction between water and the lone pairs of the azolyl rings.

In the solid state (CPMAS-NMR spectra), the ^{13}C chemical shifts are similar to those in solution, but always split. The splitting is due to either disorder (**2b**[111]) or to nonequivalence of the different azolyl residues in the borate (**1c**[7]; cf. also to the splitting of the C–H and B–H stretching frequencies in the case of nonequivalent azolyl residues[14]).

C–H···O Bonding in Transition-Metal Structrures of Poly(triazolyl)borato Ligands 1b and 2b: From the ^1H NMR data of the poly(azolyl)borato anions, a significant downfield shift of the proton resonances of the azolyl rings with increasing nitrogen content becomes apparent and can be correlated to an increase in the positive polarization of the hydrogen atom (Table 6). At

Table 6. ^1H NMR chemical shifts (δ) and AM1-calculated net atomic charges (in italics) of (pyrazolyl)borates **1a** and **2a**, (triazolyl)borates **1b** and **2b**, and (tetrazolyl)borate **1c** (for numbering see Table 4) [a].

Compd	Solvent	H-3	H-4	H-5	Ref.
1a	[D$_6$]DMSO	7.21	5.90	7.31	[15]
1a	D_2O	7.54	6.25	7.67	[15]
		0.139	*0.126*	*0.156*	
2a	[D$_6$]DMSO	7.36	6.05	7.24	[15]
2a	D_2O	7.65	6.31	7.39	[15]
		0.146	*0.132*	*0.166*	
1b	[D$_6$]DMSO	7.64	–	7.95	this work
1b	D_2O	7.92	–	8.26	[13]
		0.170	–	*0.186*	
2b	[D$_6$]DMSO	7.81	–	8.09	this work
2b	D_2O	7.98	–	8.12	[11]
		0.178	–	*0.196*	
1c	[D$_6$]DMSO	–	–	8.82	this work
1c	D_2O	–	–	8.83	[7]
				0.201	

[a] The relationships between the chemical shifts in the two solvents can be expressed as $\delta(DMSO) = -0.88 + 1.08\,\delta(D_2O)$ with a correlation coefficient $r^2 = 0.985$. The value of r^2 and the fact that the slope is near 1 indicates that ^1H NMR is unable to distinguish between specific solvation by H_2O (through O–H···N hydrogen bonds) and general solvent effects (Onsager type). If specific solvent effects were clearly apparent, water should affect the signals of protons of the most basic compounds to a greater extent [here: the (pyrazolyl)borates]. The correlation between ^1H chemical shifts and the corresponding net atomic charges [q(AM1)] of the protons is acceptable; $\delta(DMSO) = 2.4 + 30.4\,q(AM1)$ (with $r^2 = 0.847$) and $\delta(D_2O) = 3.3 + 26.8\,q(AM1)$ (with $r^2 = 0.787$).

the same time, the structures of the transition-metal complexes with the poly(azolyl)borato ligands **1b**, **2b**, and **1c** often contain a considerable number of water molecules both as metal ligands and as water of crystallization. The incorporation of the water of crystallization stems from the presence of the additional nitrogen donor atoms and the formation of O–H···N bonds.[8, 10, 12–14] These effects lead to the presence of C–H···O bonds, whose energetic contribution is known to be small, yet they can be major determinants of crystal packing with their strength and effectiveness depending on the C–H carbon acidity.[46, 47] Typical H···O distances lie somewhere between 2.00 and 2.80 Å, accompanied by large C–H···O angles of between 150 and 180°. An H···O value of 2.80 Å is often employed as a cut-off in the study of C–H···O hydrogen bonding, however, even longer values can be considered. Small C–H···O angles for bent hydrogen bonds are also observed.[46] Figure 8 shows a plot of the C–H···O angle versus

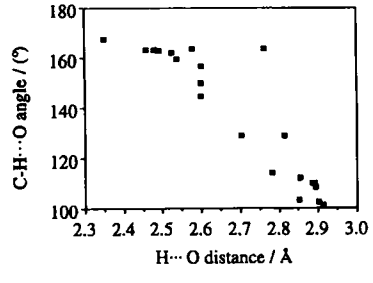

Fig. 8. Plot of C–H···O angle versus H···O distance for intra- and intermolecular C–H···O hydrogen bonds in transition-metal poly(azolyl)-borato complexes (azolyl = 1,2,4-triazolyl or tetrazolyl).

0947-6539/96/0208-0998 $ 15.00+.25/0 Chem. Eur. J. 1996, 2, No. 8

the H···O distance for intra- and intermolecular hydrogen bonds in transition-metal poly(azolyl)borato complexes found in the X-ray structures of $[M\{HB(C_2H_2N_3)_3\}_2]\cdot 6H_2O$ (M = Zn, Ni),[12,13] $^1_\infty\{[Mn\{HB(C_2H_2N_3)_3\}_2(H_2O)_2]\cdot 4H_2O\}$,[14] $\{[M\{H_2B(C_2H_2N_3)_2\}_2(H_2O)_2]\cdot nH_2O\}$ (M = Mn, $n = 4$; Ni, $n = 2$; Cu, $n = 6$),[13,14] and $^2_\infty\{[Cd\{H_2B(CHN_4)_2\}_2(H_2O)_2]\cdot 2H_2O\}$.[8] There is a large angular distribution (100–170°) when longer H···O separations (>2.70 Å) are included. As the H···O separation narrows the C–H···O angle focuses around 160°, however. The role played by these C–H···O and by additional C–H···N interactions in determining molecular packing and conformation in these poly(azolyl)borate structures will be analyzed in detail elsewhere.

Conclusions

It has been shown by comparative cyclovoltammetric and photoelectron spectroscopy studies on the iron and cobalt complexes of hydrotris(pyrazolyl)- and -(triazolyl)borate that the (triazolyl)borato ligand has the effect of decreasing the energy of the filled orbitals through a decrease in π-donor and, to a smaller extent, σ-donor bond strength. This "electron withdrawing" effect of the additional ring nitrogen could be followed by semiempirical AM1 and INDO/S MO calculations on the free ligands and the transition-metal complexes. At the same time, the change in the ligand-field splitting amounts to a fine-tuning effect, as seen by the similarity of the UV/Vis spectra and the shift in transition temperatures in the spin equilibrium of the homoleptic hydrotris(azolyl)boratoiron(II) complexes (azolyl = pyrazolyl and 1,2,4-triazolyl). The low-spin/high-spin transition was followed by differential scanning calorimety, temperature-variable UV/Vis, and ^{57}Fe Mössbauer spectroscopy to give a transition temperature of about 65 °C for compound **3b**.

^{15}N NMR was used to investigate the electronic differences between the nitrogen atoms in the azolyl rings in the poly(azolyl)borato anions $H_{4-n}B(azolyl)_n^-$ (azolyl = pyrazolyl, n = 2,3; 1,2,4-triazolyl, n = 2,3; tetrazolyl, n = 2) and supports the assignment of a higher negative charge to the exodentate (N-4) versus the endodentate (N-2, N-3) nitrogen atoms.

The additional ring nitrogen atoms lead to the incorporation of water and slightly increase the C–H acidity (from ^{1}H NMR) such that C–H···O hydrogen bonds can be observed in a number of poly(azolyl)borate transition-metal structures (azolyl = 1,2,4-triazolyl and tetrazolyl).

Experimental Procedure

The potassium salts of **1a** [6], **2a** [6], **1b** [13], **2b** [9,48], and **1c** [7], and the iron and cobalt complexes **3a** and **4a** [6] and **3b** and **4b** [11] were prepared as described in the literature. UV/Vis: Beckman 750. DSC: Mettler.

Cyclovoltammetry: Electrochemical Analyzer BAS 100 B with cell arrangement C-2 (Bioanalytical Systems, USA). Three-electrode system with Pt-disk working electrode (electrode area 2.27 mm^2), Ag/AgCl reference electrode (3 M), and platinum wire auxiliary electrode; range: −1.90 to +1.90 V; scan rate: 100 mVs^{-1}; supporting electrolyte: 0.1 M $[n$Bu$_4$N$][ClO_4]$ in CH_2Cl_2; depolarizer: 10^{-3} M **3a**, **3b**, **4a**, **4b** in supporting electrolyte.

Photoelectron spectroscopy: He I and He II photoelectron spectra of **3a**, **4a**, **3b**, and **4b** were measured on a PES Laboratories 0078 PE spectrometer equipped with a hollow cathode discharge lamp. The spectra were collected by repeated scans accumulated on an Atari microprocessor. The spectra were calibrated with reference to N_2, Xe, and He. The results obtained for **3a** and **4a** were consistent with those of Bruno et al. [22,23].

Mössbauer spectroscopy: ^{57}Fe Mössbauer spectra were collected in constant acceleration modus with a ^{57}Co(Rh) source (AMERSHAM). The specimen (in a boron nitride holder) was placed in a continuously controlled oven furnace at low pressure; the source was at room temperature and normal pressure. The transmission of the γ-radiation was detected by means of a NaI(Tl) scintillation counter. The actual velocity of the system was measured with an He–Ne Laser interferometer. Both the velocity information and the intensities were digitalized synchronously by means of a multichannel analyzer in each of the 1024 data channels. The δ scale is related to the shift of α-iron as origin of the ordinate. The sample of **3b** was carefully ground to a fine powder in a mortar. The iron contamination in the beam, especially in the beryllium windows of the detector was taken into account with two fixed base lines. The experimental curve fit was carried out iteratively with a Fortran fit program [49] using the least-squares method in a thin absorber approximation with symmetrical Lorentz functions. The spectral parameters ($\delta^{\alpha-Fe}$, $\Gamma/2$, and possibly ΔE_Q) could each be fixed or correlated in groups in the case of a multiline fit. Fits were aimed for with largely open parameters.

NMR spectrosopy: The ^{1}H, ^{13}C, and ^{15}N (in [D$_6$]DMSO) NMR spectra in solution were recorded on a Bruker AC200 instrument (UNED) working at 200.13 (^{1}H), 50.32 (^{13}C), or (20.29) MHz (^{15}N). The ^{15}N NMR spectra in D_2O were collected on a Bruker ARX400 instrument at 40.54 MHz. ^{1}H and ^{13}C chemical shifts (δ) from internal TMS with an accuracy of 0.01 (for ^{1}H) and 0.1 (for ^{13}C NMR); coupling constants (J) accurate to ±0.3 and ±0.6 Hz, respectively (for the standard conditions used see ref. [50]). ^{15}N NMR spectra were obtained in 10 mm NMR tubes; the concentration was 10–25% (w/v). For the samples in [D$_6$]DMSO, nitromethane was used as an external standard: pure nitromethane was present in a coaxial tube (5 mm) centered inside a 10 mm tube containing pure [D$_6$]DMSO. No corrections for bulk differences were applied. INVGATE typical conditions were as follows: pulse angle 15.0; spectral width 15.6 kHz; data points, 16 or 32 K, pulse repitition time (D1) 10 or 20 s; continuous broad-band proton decoupling. In all cases, it was necessary to accumulate 5000–10000 transients in order to obtain spectra with an acceptable signal-to-noise ratio. ^{1}H–^{15}N coupling constants of compound **1b** in DMSO were obtained by using the INEPT sequence D1 = 2.0, D2 = 0.008, Hz/pt = 1.9. The spectra in D_2O were originally measured against a saturated aqueous solution of $^{15}NH_4{}^{15}NO_3$ with $\delta(NH_4) = -359.5$ from neat CH_3NO_2. The ^{15}N NMR spectra in D_2O were measured by using the INEPT pulse sequence with typical conditions as follows: acquisition time 0.65538 s, FID resolution 0.76 Hz, dwell time 10.0 μs; proton coupled; parameter for polarization transfer, delay D4 with $\tau = 1/[4J(N,H)] = 0.0179$ s, based on an average assumed coupling of J(N,H) of 14 Hz.

The high-resolution solid-state ^{13}C NMR spectra were obtained at room temperature on the Bruker AC200 spectrometer under conditions of cross-polarization (CP) and magic-angle spinning (MAS) with a 7 mm Bruker DAB7 probe head with rotation frequencies of about 3.5–4.5 kHz. Samples were carefully packed in ZrO_2 rotors (ca. 200 mg of material). The standard CPMAS pulse sequence was applied with a 7 μs ^{1}H-90° pulse width, 1 ms contact pulses, and 3 s repitition time, the spectral width being 15000 Hz. All chemical shifts are given with respect to the spectrometer reference frequency, which was calibrated by the glycine signal at $\delta = 176.1$.

Theoretical studies: Qualitative MO computations were perfomed within the extended Hückel formalism [51] with weighted H_{ij}'s [52] with the CACAO program (Version 4.0) [53]. Geometrical parameters were taken from the X-ray structural work of **3a,b** and **4a,b** [10,54]; the atomic parameters were used as supplied by the CACAO program.

Semiempirical AM1 [55] and INDO/S [56] calculations were carried out with the HyperChem computational package (Version 3.0, Autodesk Inc., Sausolito, CA 94965, USA) on AM1 or INDO/1 geometry-optimized structures. The AM1 method was used for the poly(azolyl)borato ligands, while the INDO/1,S method was employed for the transition-metal complexes. For the iron complexes **3a** and **b** geometry optimization was carried out on the singlet state.

Acknowledgements: This work was supported by the Deutsche Forschungsgemeinschaft (grant Ja466/4-1), the Fonds der Chemischen Industrie, and the Gesellschaft der Freunde der TU Berlin. We express our appreciation and thanks to Prof. H. Schumann for his continuous and generous support. A copy of the CACAO program was kindly provided by Dr. D. M. Proserpio. We thank Dipl.-Chem. D. Blunk for the DSC measurement and one of the referees for helpful comments.

Received: December 11, 1996 [F264]

[1] Reviews: S. Trofimenko, *Chem. Rev.* **1993**, *93*, 943–980; I. Santos, N. Marques, *New J. Chem.* **1995**, *19*, 551–571. P. K. Byers, A. J. Canty, R. T. Honeyman, *Adv. Organomet. Chem.* **1992**, *34*, 1–65. K. Niedenzu, S. Trofimenko, *Topics Curr. Chem.* **1986**, *131*, 1–37; S. Trofimenko, *Progr. Inorg. Chem.* **1986**, *34*, 115–210.

[2] For recent examples see: E. H. Ha, R. Y. N. Ho, J. F. Kisiel, J. S. Valentine, *Inorg. Chem.* **1995**, *34*, 2265–2266. K. Yang, Y. Yin, D. Jin, *Polyhedron* **1995**, *14*, 1021–1023. U. Hartmann, H. Vahrenkamp, *Chem. Ber.* **1994**, *127*, 2381–2385. N. Kitajima, N. Tamura, H. Amagai, H. Fukui, Y. Morooka, Y. Mizutani, T. Kitagawa, R. Mathur, K. Heerwegh, C. A. Reed, C. R. Randall, L. Que, Jr., K. Tatsumi, *J. Am. Chem. Soc.* **1994**, *116*, 9071–9085. N. Kitajima, Y. Moro-oka, *J. Chem. Soc. Dalton Trans.* **1993**, 2665–2671. R. Alsfasser, M. Ruf, S. Trofimenko, H. Vahrenkamp, *Chem. Ber.* **1993**, *126*, 703–710.

[3] See for example: O. Renn, L. M. Venanzi, A. Marteletti, V. Gramlich, *Helv. Chim. Acta* **1995**, *78*, 993–1000. K. Yoon, G. Parkin, *Polyhedron* **1995**, *14*, 811–821. A. L. Rheingold, B. S. Haggerty, S. Trofimenko, *J. Chem. Soc. Chem. Commun.* **1994**, 1973–1974. M. Ruf, K. Weis, H. Vahrenkamp, *ibid.* **1994**, 135–136. M. Etienne, F. Biasotto, R. Mathieu, *ibid.* **1994**, 1661. A. Frazer, B. Piggott, M. B. Hursthouse, M. Mazid, *J. Am. Chem. Soc.* **1994**, *116*, 4127–4128. L. Hasinoff, J. Takats, X. W. Zhang, A. H. Bond, R. D. Rogers, *ibid.* **1994**, *116*, 8833–8834. O. M. Reinaud, A. L. Rheingold, K. H. Theopold, *Inorg. Chem.* **1994**, *33*, 2306–2308. Y. Sun, R. McDonald, J. Takats, V. W. Day, T. A. Eberspacher, *ibid.* **1994**, *33*, 4433–4434; and references therein.

[4] Effects of an isolobal C–H → E substitution are also studied in other compounds, e.g. in (hetero)cyclopentadienyl ligands or in (hetero)benzenes. See, for example, a) C. Janiak, U. Versteeg, K. C. H. Lange, *J. Organomet. Chem.* **1995**, *501*, 219–234. b) C. Janiak, N. Kuhn, R. Gleiter, *J. Organomet. Chem.* **1994**, *475*, 223–227. c) C. Janiak, N. Kuhn, *Advances in Nitrogen Heterocycles*, Vol. II (Ed.: C. J. Moody), JAI Press, Greenwich, CT, USA, **1996**, pp. 179–210. A. J. Ashe III, S. Al-Ahmed, S. Pilotek, D. B. Puranik, C. Elschenbroich, A. Behrendt, *Organometallics* **1995**, *14*, 2689–2698. A. J. Ashe III, *Top. Curr. Chem.* **1982**, *105*, 125–155.

[5] Attempts to obtain the tris(tetrazolyl)borate and the tetrakis(1,2,4-triazolyl)- or tetrakis(tetrazolyl)borate by the Trofimenko or KBH_4 method [6] have failed so far in our hands. Tetrazole and triazole decompose at the temperatures required for tri or tetra substitution [7,8].

[6] S. Trofimenko, *Inorg. Synth.* **1970**, *12*, 99–106.

[7] C. Janiak, L. Esser, *Z. Naturforsch. B* **1993**, *48*, 394–396.

[8] C. Janiak, T. G. Scharmann, K.-W. Brzezinka, P. Reich, *Chem. Ber.* **1995**, *128*, 323–327.

[9] G. G. Lobbia, F. Bonati, P. Cecchi, *Synth. React. Inorg. Met.-Org. Chem.* **1991**, *21*, 1141–1151.

[10] C. Janiak, *J. Chem. Soc. Chem. Commun.* **1994**, 545–547.

[11] C. Janiak, *Chem. Ber.* **1994**, *127*, 1379–1385.

[12] C. Janiak, H. Hemling, *J. Chem. Soc. Dalton Trans.* **1994**, 2947–2952.

[13] C. Janiak, T. G. Scharmann, H. Hemling, D. Lentz, J. Pickardt, *Chem. Ber.* **1995**, *128*, 235–244.

[14] C. Janiak, T. G. Scharmann, W. Günther, F. Girgsdies, H. Hemling, W. Hinrichs, D. Lentz, *Chem. Eur. J.* **1995**, *1*, 637–644.

[15] C. Lopez, R. M. Claramunt, D. Sanz, C. Foces-Foces, F. H. Cano, R. Faure, E. Cayon, J. Elguero, *Inorg. Chim. Acta* **1990**, *176*, 195–204.

[16] J. P. Jesson, S. Trofimenko, D. R. Eaton, *J. Am. Chem. Soc.* **1967**, *89*, 3148–3158.

[17] P. R. Sharp, A. J. Bard, *Inorg. Chem.* **1983**, *22*, 2689–2693.

[18] Electrochemical studies on **3a,b** and **4a,b** in water gave only irreversible responses and electrode poisoning. P. Zanello, University of Siena, Italy, private communication.

[19] J. Heinze, *Angew. Chem.* **1984**, *96*, 823–840; *Angew. Int. Ed. Engl.* **1984**, *23*, 831–847.

[20] S. Zamponi, G. Gambini, P. Conti, G. G. Lobbia, R. Marassi, M. Berrettoni, B. Cecchi, *Polyhedron* **1995**, *14*, 1929–1935.

[21] W. H. Armstrong, A. Spool, G. Papaefthymiou, R. B. Frankel, S. J. Lippard, *J. Am. Chem. Soc.* **1984**, *106*, 3653–3667.

[22] G. Bruno, E. Cilberto, I. Fragalá, G. Granozzi, *Inorg. Chim. Acta* **1981**, *48*, 61–64.

[23] G. Bruno, G. Centineo, E. Cilberto, S. Di Bella, I. Fragalá, *Inorg. Chem.* **1984**, *23*, 1832–1836.

[24] S. Cradock, R. H. Findlay, M. H. Palmer, *Tetrahedron* **1973**, *29*, 2173–2181.

[25] T. Buchen, P. Gütlich, *Inorg. Chim. Acta* **1995**, *231*, 221–223.

[26] S. Calogero, G. G. Lobbia, P. Cecchi, G. Valle, J. Friedl, *Polyhedron* **1994**, *13*, 87–97.

[27] J.-P. Martin, J. Zarembowitch, A. Dworkin, J. G. Haasnoot, E. Codjovi, *Inorg. Chem.* **1994**, *33*, 2617–2623.

[28] P. Gütlich, A. Hauser, H. Spiering, *Angew. Chem.* **1994**, *106*, 2109–2141; *Angew. Chem. Int. Ed. Engl.* **1994**, *33*, 2024–2054.

[29] F. Grandjean, G. J. Long, B. B. Hutchinson, L. Ohlhausen, P. Neill, J. D. Holcomb, *Inorg. Chem.* **1989**, *28*, 4406–4414.

[30] G. J. Long, B. B. Hutchinson, *Inorg. Chem.* **1987**, *26*, 608–613.

[31] T. G. Gibb, *Spectroscopy*, Vol. 1 (Eds.: B. P. Straughan, S. Walker), Chapman and Hall, London, **1976**, pp. 255–292. V. I. Goldanskii, V. V. Khrapov, R. A. Stukan, *Organomet. Chem. Rev A.* **1969**, *4*, 225–261. A. Vértes, L. Korecz, K. Burger, *Mössbauer Spectroscopy*, Elsevier, Amsterdam, **1979**, pp. 144–160.

[32] Y. Sohrin, H. Kokusen, M. Matsui, *Inorg. Chem.* **1995**, *34*, 3928–3934.

[33] J. P. Jesson, S. Trofimenko, D. R. Eaton, *J. Am. Chem. Soc.* **1967**, *89*, 3158–3164. J. P. Jesson, J. F. Weiher, *J. Chem. Phys.* **1967**, *46*, 1995–1996. J. P. Jesson, J. F. Weiher, S. Trofimenko, *ibid.* **1968**, *48*, 2058–2066. G. J. Long, B. B. Hutchinson, *Inorg. Chem.* **1987**, *26*, 608–613. A. Gulino, E. Ciliberto, S. Di Bella, I. Fragalà, *Inorg. Chem.* **1993**, *32*, 3759–3761. B. Hutchinson, L. Daniels, E. Henderson, P. Neill, G. J. Long, L. W. Becker, *J. Chem. Soc. Chem. Commun.* **1979**, 1003–1004.

[34] In ref. [33b] $\lambda = 535$ nm was given for the d–d transition in **3a** in CH_2Cl_2.

[35] M. Witanowski, L. Stefaniak, G. A. Webb, *Annu. Rep. NMR Spectrosc.* (Ed.: G. A. Webb), Academic Press, London, **1986**, *18*, 68–72, 122–131; **1981**, *11B*, 32–36, 74–84.

[36] R. K. Harris, *Nuclear Magnetic Resonance Spectroscopy*, Pitman, London, **1983**, Chap. 5–14, pp. 138–141.

[37] L. Stefaniak, J. D. Roberts, M. Witanowski, G. A. Webb, *Org. Magn. Reson.* **1984**, *22*, 215–220.

[38] A correlation between nitrogen chemical shifts and electron density has been demonstrated in methylanilines: G. Adler, R. L. Lichter, *J. Org. Chem.* **1974**, *39*, 3547–3551.

[39] For more detailed and comprehensive nitrogen chemical shift calculations, see for example: B. N. Lamphun, G. A. Webb, M. Witanowski, *Org. Magn. Reson.* **1983**, *21*, 501–504. M. Jallali-Heravi, G. A. Webb, *J. Magn. Reson.* **1978**, *32*, 429–439. K. A. K. Ebraheem, G. A. Webb, *Progr. NMR Spectrosc.* (Eds.: J. Emsley, J. Feeney, L. H. Sutcliffe), Pergamon Press, Oxford, **1977**, *11*, 149–181. M. Witanowski, L. Stefaniak, H. Januszewski, G. A. Webb, *Tetrahedron* **1971**, *27*, 3129–3141.

[40] Good results were only obtained for tetrazoles: E. Bojarska-Olejnik, L. Stefaniak, M. Witanowski, G. A. Webb, *Bull. Chem. Soc. Jpn.* **1986**, *59*, 3263. V. M. Naumenko, A. O. Koren, P. N. Gaponik, *Magn. Res. Chem.* **1992**, *30*, 558.

[41] I. I. Schuster, J. D. Roberts, *J. Org. Chem.* **1979**, *44*, 3864–3867. I. I. Schuster, C. Dyllick-Brenzinger, J. D. Roberts, *ibid.* **1979**, *44*, 1765–1768.

[42] Mn^{II}: S. Gorter, D. W. Engelfriet, *Acta Crystallogr. Sect. B* **1981**, *37*, 1214–1218. Fe^{III}: W. L. Driessen, R. A. G. Graaff, J. G. Vos, *Acta Crystallogr. Sect. B* **1983**, *39*, 1635–1637. Cu^{II}: Yu. L. Slovokhotov, Yu. T. Struchkov, A. S. Polinsky, V. S. Pshezhetsky, T. G. Ermakova, *Cryst. Struct. Commun.* **1981**, *10*, 577–582.

[43] D. S. Moore, S. D. Robinson, *Adv. Inorg. Chem.* **1988**, *32*, 171–239.

[44] a) J. Catalán, J. L. M. Abboud, J. Elguero, *Adv. Heterocycl. Chem.* **1987**, *41*, 187–274. b) R. M. Claramunt, D. Sanz, G. Boyer, J. Catalán, J. L. G. de Paz, J. Elguero, *Magn. Reson. Chem.* **1993**, *31*, 791–800.

[45] J. Elguero, M. Gil, N. Iza, C. Pardo, M. Ramos, *Appl. Spectrosc.* **1995**, *49*, 1111–1119 and references therein.

[46] D. Braga, F. Grepioni, K. Biradha, V. R. Pedireddi, G. R. Desiraju, *J. Am. Chem. Soc.* **1995**, *117*, 3156–3166 and references therein.

[47] T. Steiner, W. Saenger, *J. Am. Chem. Soc.* **1993**, *115*, 4540–4547. G. R. Desiraju, *Acc. Chem. Res.* **1991**, *24*, 290–296. Z. Berkovitch-Yellin, L. Leiserowitz, *Acta Crystallogr.* **1984**, *B40*, 159–165.

[48] S. Trofimenko, *J. Am. Chem. Soc.* **1967**, *89*, 3170–3177.

[49] B. Fricke, *Description of a Fortran IV Fit-Program for the Fitting of Mössbauer Curves*, TH Darmstadt, Institute for Technical Nuclear Physics, lab report no. 27, **1966**. H. Bokemeyer, S. Meyer, K. Wohlfahrt, W. Wurtinger, *Program Description for the Mössbauer Fit Program "Moeve"*, TH Darmstadt, Institute for Technical Nuclear Physics, lab report no. 49, **1971**. R. Karl, Dissertation, TU Berlin, **1978**. J. Kähler, Dissertation, TU Berlin, **1984**.

[50] R. M. Claramunt, D. Sanz, J. Catalán, F. Fabero, N. A. García, C. Foces-Foces, A. L. Llamas-Saiz, J. Elguero, *J. Chem. Soc. Perkin Trans. 2* **1993**, 1687–1699.

[51] R. Hoffmann, *J. Chem. Phys.* **1963**, *39*, 1397–1412; R. Hoffmann, W. N. Lipscomb, *ibid.* **1962**, *36*, 2179–2189; **1962**, *37*, 2872–2883.

[52] J. H. Ammeter, H.-B. Bürgi, J. C. Thibeault, R. Hoffmann, *J. Am. Chem. Soc.* **1978**, *100*, 3686–3692.

[53] C. Mealli, D. M. Proserpio, *J. Chem. Educ.* **1990**, *67*, 399–402.

[54] J. D. Oliver, D. F. Mullica, B. B. Hutchinson, W. O. Milligan, *Inorg. Chem.* **1980**, *19*, 165. M. R. Churchill, K. Gold, C. E. Maw, *ibid.* **1970**, *9*, 1597.

[55] J. J. P. Stewart, *Reviews in Computational Chemistry* (Eds.: K. B. Lipkowitz, D. B. Boyd), VCH, Weinheim, **1990**, Chap. 2, pp. 45–81.

[56] A. D. Bacon, M. C. Zerner, *Theor. Chim. Acta* **1979**, *53*, 21–54. M. C. Zerner, *Reviews in Computational Chemistry II* (Eds.: K. B. Lipkowitz, D. B. Boyd), VCH, Weinheim, **1991**, pp. 313–365. M. C. Zerner, G. H. Loew, R. F. Kirchner, U. T. Mueller-Westerhoff, *J. Am. Chem. Soc.* **1980**, *102*, 589–599.

0947-6539/96/0208-1000 $ 15.00+.25/0